

Mechanical properties of metallic glass matrix composites: Effects of reinforcement character and connectivity

X.L. Fu,^a Y. Li^{a,b} and C.A. Schuh^{c,*}

^aSingapore–MIT Alliance, National University of Singapore, Lower Kent Ridge Road, Singapore 119260, Singapore

^bDepartment of Materials Science and Engineering, Faculty of Engineering, Engineering Drive 1, National University of Singapore, Singapore 117576, Singapore

^cDepartment of Materials Science and Engineering, Massachusetts Institute of Technology, Cambridge, MA 02139, USA

Received 29 November 2006; accepted 11 December 2006

Available online 8 January 2007

We present a systematic study of the room-temperature mechanical behavior of in situ Zr-based bulk metallic glass matrix composites over the full range of reinforcement volume fractions ($f = 0$ –100%). In line with prior work, our data show a transition where the deformation behavior is governed by the properties of the glassy matrix at low f and by those of the reinforcement phase at high f . However, unlike the situation in ductile-phase reinforced glasses, where percolation of the second phase is apparently beneficial, we show that a high volume fraction of brittle reinforcement is undesirable.

© 2006 Acta Materialia Inc. Published by Elsevier Ltd. All rights reserved.

Keywords: Metallic glasses; Composites; Toughness; Ductility; Percolation

Recent years have seen rapid progress in the development of in situ composites based on glass-forming alloys [1–7]. The resulting bulk metallic glass matrix composites (BMGMCs) contain micrometer-scale reinforcements which are meant to disrupt shear localization, while maintaining the high strength (up to several GPa) and large elastic strain limit ($\sim 2\%$) of a bulk metallic glass. A variety of alloy systems exhibit the possibility of in situ second phase formation, and the resulting BMGMCs sometimes show signatures of improved toughness – most notably improved compressive malleability [1–5]. However, not all of the BMGMCs exhibit obviously improved plasticity or toughness [2,3,5,8], and it remains unclear what factors separate success from failure in this respect. In fact, true tensile extensibility (“ductility”) at room temperature has only been reported twice to our knowledge in BMGMCs: the original work of Johnson and co-workers showed an improved tensile fracture strain to about 5% [1] as well as improved toughness [9] in a Zr-based BMGMC, and subsequently Lee et al. [2] reported 6% tensile ductility in a La-based BMGMC. There are two common fea-

tures of these successful studies, both of which might contribute to the observed tensile ductility:

- (i) In both of the two ductile composites, a high volume fraction of the second phase was present. In fact, the study of Lee et al. [2] further showed, by varying the volume fraction of reinforcement, that a volume fraction above a critical level was required to achieve improved plasticity (possibly owing to percolation of the second phase).
- (ii) In both studies, the reinforcement phases were inherently ductile crystalline metal phases (nearly pure La in Ref. [2], and a body-centered cubic Zr–Ti–Nb phase in Refs. [1,9]).

Because both of the above BMGMCs contained a ductile reinforcement and involved a high volume fraction, it is not clear whether one or both of these properties are required to improve plasticity in the composites. Our purpose in this letter is to isolate these two variables by examining a different composite-forming system, and to show that whereas a percolating ductile phase may “ductilize” a BMGMC, reinforcement percolation must be avoided if the second phase is inherently brittle.

Seven different alloy compositions were used in this work: $Zr_{49}Cu_{45}Al_6$ is a bulk glass former and $Zr_{50}Cu_{(50-x)}Al_x$ (with $x = 8, 10, 12, 13, 14, 16$) are a series of in situ BMGMCs with different volume fractions of reinforcement. Some processing and characterization

* Corresponding author. Tel.: +1 617 452 2659; e-mail: schuh@MIT.EDU

details of similar alloys are available in Ref. [10], and we have used similar procedures here. All the alloys were prepared by arc-melting a mixture of Zr (99.9% purity), Cu (99.99%) and Al (99.9%) in an Ar atmosphere, and casting into a copper mold to produce rods 5 mm in diameter and 56 mm in length. As depicted in Figure 1, the different alloys contain various volume fractions, f , of second phase dendrites formed in situ during casting. Quantitative image analysis revealed that f increases with Al content. Unlike prior studies that systematically vary f in situ BMGMCs [2,4,7,11], the alloys in this work span the full range of $f = 0$ –100% (cf. Fig. 1).

Polished cross-sections of the as-cast rods were examined by conventional X-ray diffractometry (XRD), using a Bruker analytical X-ray system, as shown in Figure 2. As the reinforcement volume fraction increases from $f = 0\%$ upwards, crystalline peaks for the τ_3 ($\text{Zr}_{51}\text{Cu}_{29}\text{Al}_{20}$) phase gradually come to dominate the pattern, replacing the amorphous halo of the base glass composition. In the sample with $f = 100\%$, not only is the τ_3 phase present, but there is also some indication that two additional crystalline phases – ZrCu and τ_5 ($\text{Zr}(\text{CuAl})_2$) – are present in smaller quantities. In the latter alloy there is no obvious evidence for any amorphous content. It is important to note that the dominant reinforcement phase in these BMGMCs is the intermetallic τ_3 phase, which is expected to be hard and brittle.

The experimental alloys were characterized by differential scanning calorimetry (DSC), using a TA instruments 2920 modulated DSC, with a heating rate of 20 K min^{-1} . The onset glass transition temperature (T_g^{onset}) and heat of crystallization (ΔH_x) are shown in Table 1. T_g^{onset} increases slightly as the volume percentage increases (in line with a report for similar Zr-based BMGMCs [11]), while ΔH_x decreases as f increases.

We have used two mechanical tests which provide qualitative indications about the strength and brittleness of these BMGMCs. First, we used standard Vicker's indentations made by a Zwick/Roell Indentec apparatus, applying 30 and 10 kgf loads on polished cross-sections of each alloy; these loads produced impressions substantially larger than the characteristic size of the reinforcements shown in Figure 1, insuring that each measurement properly sampled the composite properties and not those of a single phase. In addition to measuring

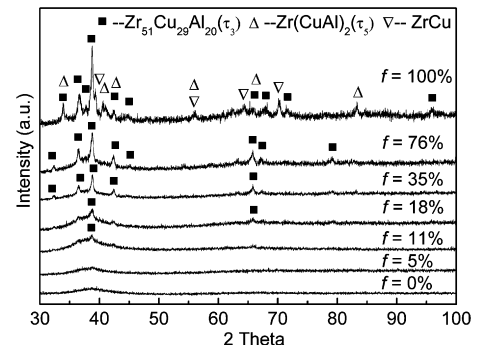


Figure 2. X-ray diffraction patterns of the monolithic amorphous alloy ($f = 0$) and bulk metallic glass matrix composites.

Table 1. Composition, reinforcement volume fraction and thermal analysis results for monolithic amorphous alloy ($f = 0\%$) and composites with $f = 5\%$, 11% , 18% , 35% , 76% and 100%

Composition	f (%)	T_g^{onset} (K)	T_g^{end} (K)	T_x (K)	ΔH_x (J g^{-1})
$\text{Zr}_{49}\text{Cu}_{45}\text{Al}_6$	0	694	709	755	58
$\text{Zr}_{50}\text{Cu}_{42}\text{Al}_8$	5	695	711	768	49
$\text{Zr}_{50}\text{Cu}_{40}\text{Al}_{10}$	11	703	720	770	41
$\text{Zr}_{50}\text{Cu}_{38}\text{Al}_{12}$	18	705	725	773	40
$\text{Zr}_{50}\text{Cu}_{37}\text{Al}_{13}$	35	706	728	778	38
$\text{Zr}_{50}\text{Cu}_{36}\text{Al}_{14}$	76	711	726	771	18
$\text{Zr}_{50}\text{Cu}_{34}\text{Al}_{16}$	100	n.a.	n.a.	n.a.	0

the hardness value, we also examined the resulting impressions in a scanning electron microscope (SEM), to ascertain whether tensile cracks formed around the indentation. Second, we performed standard compression testing, using polished cylindrical specimens cut from the as-cast rods with lengths of about 10 mm and diameters of about 5 mm; an applied engineering strain rate of 10^{-4} s^{-1} was used.

Vickers hardness values for all of the experimental alloys are shown in Figure 3. The hardness of the amorphous alloy ($f = 0$) is $\sim 4.8 \text{ GPa}$, which is in line with expectations [12,13] based on its compressive strength, which we measured to be in the range 1.2–1.5 GPa. As the volume percentage of reinforcements increases, the hardness climbs as high as 6.3 GPa at $f = 100\%$; this

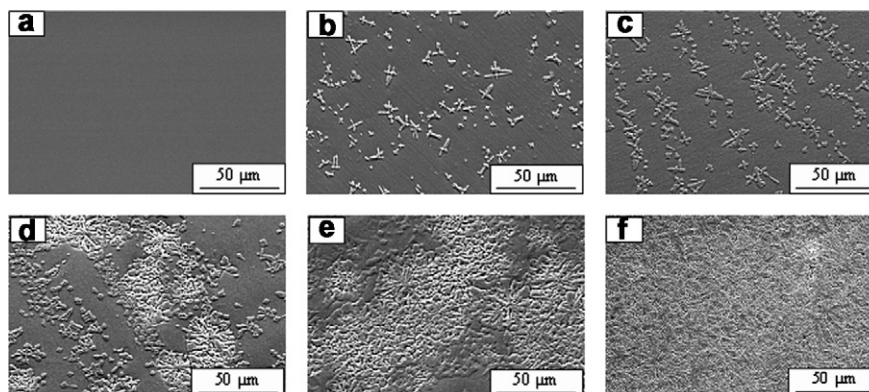


Figure 1. SEM micrographs of (a) the monolithic bulk metallic glass ($f = 0\%$) and the bulk metallic glass matrix composites with (b) $f = 11\%$, (c) $f = 18\%$, (d) $f = 35\%$, (e) $f = 76\%$ and (f) $f = 100\%$.

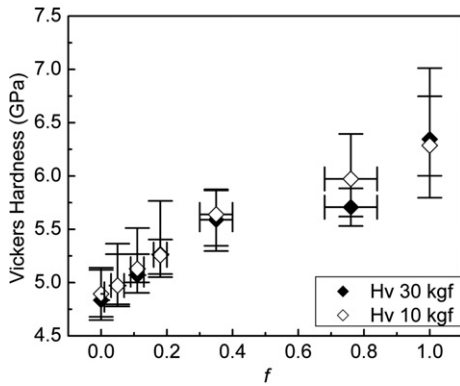


Figure 3. Variation in Vickers hardness with different reinforcement volume fractions, using both 30 and 10 kgf loads.

confirms our expectation that the intermetallic reinforcement phase is hard, even in comparison with the amorphous matrix. Referring to the SEM images of 30 kgf indents shown in Figure 4, we can also see a transition in the toughness of these specimens. For the monolithic amorphous alloy as well as the dilute composites at $f \leq 18\%$, the indents were clean, exhibited pile-up around the edges, and no cracks could be found near or around the impression site; these results are typical for indentation of BMGs [14,15], and demonstrate plastic flow without cracking. However, beginning at $f = 35\%$, small cracks can be found emanating from corners of the indentations. At $f = 35\%$, these cracks are quite small, as shown in the inset to Figure 4d, but as f increases the cracks become consistently larger (Fig. 4e). At $f = 100\%$ (fully crystalline intermetallic), large cracks are clearly evident at all four corners of the indent. For brittle materials, the lengths of the tensile corner cracks around an indentation are directly related to toughness [16,17]. Longer cracks correlate with lower fracture toughness, so the images in Figure 4 demonstrate that at higher reinforcement volume fractions, the present BMGMCs become more brittle.

Further evidence supporting the transition to more brittle behavior of high- f composites is shown in Figure

5, where we present SEM micrographs of a few selected compression specimens. In Figure 5a, a dilute composite with $f = 11\%$ is shown, exhibiting a characteristic shear failure at an inclined angle to the compression axis. The inset in Figure 5a also shows the fracture surface, on which the typical shear vein pattern is observed. The result in Figure 5a is representative of all the dilute composites ($f \leq 18\%$), which failed via localized plastic (shear) flow. On the other hand, at high volume fractions (e.g. $f = 76\%$ as shown in Fig. 5c), the compression samples all failed in a clearly brittle fashion. The sample in Figure 5c exemplifies a catastrophic compressive fragmentation typical of the highest reinforcement volume fractions. At an intermediate volume fraction of $f = 35\%$, the failed specimens tended to exhibit elements of both plastic shear flow and brittle fracture. Figure 5b illustrates both a region of shear failure, with inset (i) reflecting a shear vein pattern, as well as a transverse tensile crack, with a fracture surface in inset (ii) that is very rough and populated with microcracks.

The general trends observed in Figure 5 match those from Figure 4, and complement those from Figure 3; the second phase in these composites is a hard and brittle intermetallic. Increasing the volume fraction of the brittle second phase does not mitigate the tendency for shear localization in the glassy matrix, except by inducing the transition to a genuinely brittle fracture mode. When this result is compared with the results of Szuets et al. [1] and Lee et al. [2] described earlier, the key difference is that in the present BMGMCs the reinforcement is brittle, while in those studies it was ductile; whereas those authors observed improved ductility in their composites, we see a clearly opposite trend in ours. In fact, the present results are more reminiscent of partially devitrified metallic glasses [18–22], in which precipitated intermetallic phases (often of nanometer-scale) lead to hardening and embrittlement. However, to our knowledge the present results are the first to demonstrate a similar volume-fraction dependence for in situ BMGMCs with brittle micrometer-scale dendrite reinforcements.

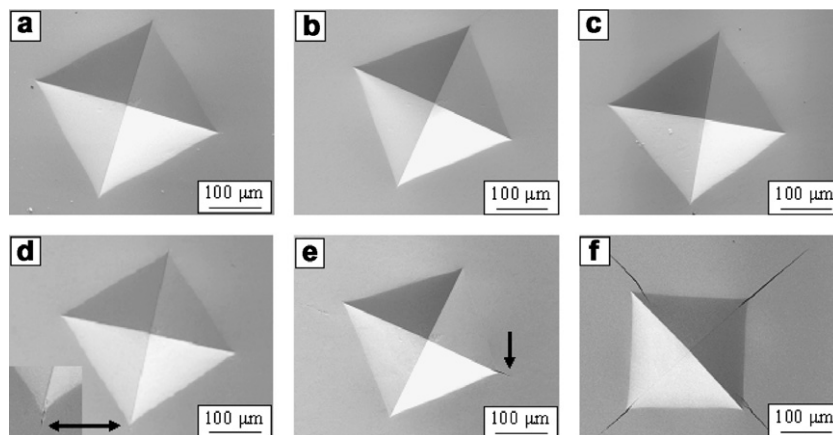


Figure 4. SEM images of Vickers indents made using 30 kgf for specimens at different reinforcement volume fractions: (a) $f = 0\%$, (b) $f = 11\%$, (c) $f = 18\%$, (d) $f = 35\%$, (e) $f = 76\%$ and (f) $f = 100\%$. The inset to (d) shows an enlargement of one of the corners of the indent where a crack was observed, and the black arrows in (d) and (e) point to indentation-induced tensile cracks.

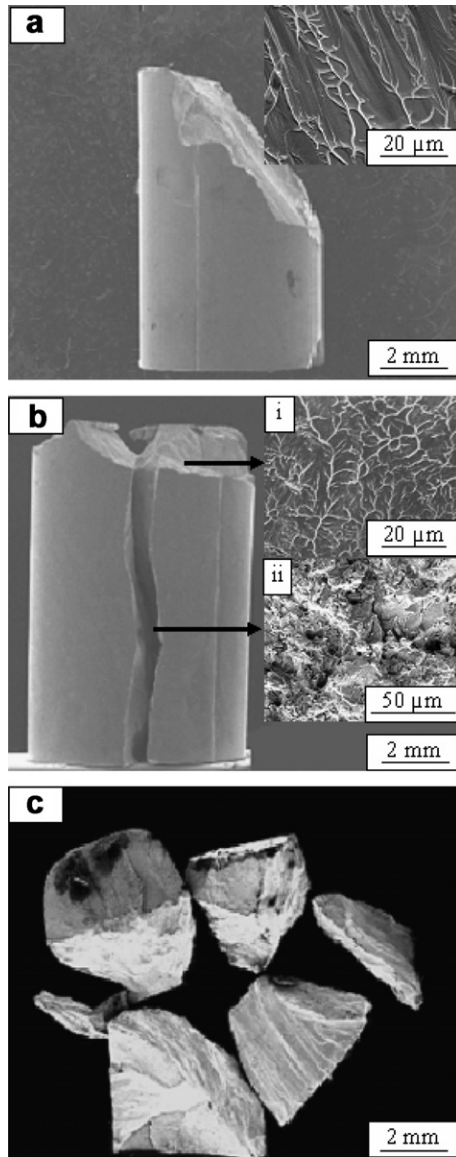


Figure 5. SEM images of selected compression samples for (a) $f = 11\%$, where the inset shows the fracture surface; (b) $f = 35\%$, where the two insets show the fracture surface from two different regions; and (c) $f = 76\%$.

A final issue worth discussing is the possibility of percolation transitions in BMGMCs. As noted earlier, Lee et al. [2] found a threshold in f in a ductile-phase reinforced BMGMC, above which ductility was observed and below which it was not. In a complementary way, our results in Figures 4 and 5 suggest that there may be a similar threshold in f for the transition to brittle behavior; BMGMCs with f below 35% exhibited no signs of a brittle fracture mode, while those above this value all did. The $f = 35\%$ composites do appear to be near a percolation condition (cf. Fig. 1d), and this value

of f is quite close to the threshold of $\sim 40\%$ identified by Lee et al. The present results are thus similar to those of Lee et al., in the sense that a critical volume fraction of second phase apparently does suppress failure by shear localization. Unfortunately, with a brittle reinforcement the alternative to shear localization is the even more detrimental brittle fracture. The present results thus suggest that for BMGMCs with micrometer-scale reinforcements, second-phase percolation is beneficial to plasticity only if the reinforcement is inherently ductile.

This work was supported by the Singapore–MIT Alliance. C.A.S. also gratefully acknowledges the support of the US Office of Naval Research under Grant N00014-04-1-0669.

- [1] F. Szuecs, C.P. Kim, W.L. Johnson, *Acta Materialia* 49 (2001) 1507.
- [2] M.L. Lee, Y. Li, C.A. Schuh, *Acta Materialia* 52 (2004) 4121.
- [3] C. Fan, R.T. Ott, T.C. Hufnagel, *Applied Physics Letters* 81 (2002) 1020.
- [4] Z. Bian, H. Kato, C.L. Qin, W. Zhang, A. Inoue, *Acta Materialia* 53 (2005) 2037.
- [5] T. Hirano, H. Kato, A. Matsuo, Y. Kawamura, A. Inoue, *Materials Transactions JIM* 41 (2000) 1454.
- [6] F.F. Wu, Z.F. Zhang, A. Peker, S.X. Mao, J. Das, J. Eckert, *Journal of Materials Research* 21 (2006) 2331.
- [7] Y. Zhang, W. Xu, H. Tan, Y. Li, *Acta Materialia* 53 (2005) 2607.
- [8] Y.F. Sun, S.K. Guan, B.C. Wei, Y.R. Wang, C.H. Shek, *Materials Science and Engineering A – Structural Materials Properties Microstructure and Processing* 406 (2005) 57.
- [9] K.M. Flores, W.L. Johnson, R.H. Dauskardt, *Scripta Materialia* 49 (2003) 1181.
- [10] D. Wang, H. Tan, Y. Li, *Acta Materialia* 53 (2005) 2969.
- [11] X.L. Fu, Y. Li, C.A. Schuh, *Applied Physics Letters* 87 (2005) 241904.
- [12] C.A. Schuh, T.G. Nieh, *Journal of Materials Research* 19 (2004) 46.
- [13] P.E. Donovan, *Journal of Materials Science* 24 (1989) 523.
- [14] J. Basu, N. Nagendra, Y. Li, U. Ramamurty, *Philosophical Magazine* 83 (2003) 1747.
- [15] C.G. Tang, Y. Li, K.Y. Zeng, *Materials Science and Engineering A – Structural Materials Properties Microstructure and Processing* 384 (2004) 215.
- [16] P.A. Hess, S.J. Poon, G.J. Shiflet, R.H. Dauskardt, *Journal of Materials Research* 20 (2005) 783.
- [17] B.R. Lawn, R. Wilshaw, *Journal of Materials Science* 10 (1975) 1049.
- [18] J.J. Lewandowski, *Materials Transactions* 42 (2001) 633.
- [19] N. Nagendra, U. Ramamurty, T.T. Goh, Y. Li, *Acta Materialia* 48 (2000) 2603.
- [20] U. Ramamurty, S. Jana, Y. Kawamura, K. Chattopadhyay, *Acta Materialia* 53 (2005) 705.
- [21] D. Deng, A.S. Argon, *Acta Metallurgica* 34 (1986) 2011.
- [22] Y.H. Kim, K. Hiraga, A. Inoue, T. Masumoto, H.H. Jo, *Materials Transactions JIM* 35 (1994) 293.